Seismic Dynamic Response Analysis of Tunnel Structures Across Fault Fracture Zones

Bin Zhi[1,a], Changwei Li[1,b], XiaoKun Li[2,c*]

[1]China Road & Bridge Corporation, Beijing, China
[2]Xi'an University of Architecture and Technology, Xi'an, China

E-mail: [a]zhib@crbc.com, [b]licw@crbc.com, [c]951180283@qq.com
*Corresponding author

Abstract. The objective of this research is to assess the seismic-induced dynamic reactions of tunnels in fault-fragmented areas and to explore efficient seismic countermeasures. Using the Tajikistan-China Highway Phase II as a reference, a numerical simulation is conducted to create a model that emulates seismic wave propagation based on collected data. The study reveals a significant increase in stress response of tunnels in the fault-fragmented region, especially near fault misalignment interfaces. The application of seismic-resistant measures has been demonstrated to greatly reduce the structural response of the tunnels. Employing damping strategies in the fault-fracture zone and its vicinity can significantly decrease both the dynamic response of the tunnel and the potential for seismic harm, highlighting the significance of such strategies in the seismic design of tunnels.

Keywords: tunnel seismicity; fault fracture zone; numerical simulation; seismic mitigation measures

1 Introduction

The seismic design of tunnels is crucial for maintaining transportation systems, enhancing safety, reducing earthquake losses, and fostering technological advancement[1,2]. Earthquakes often lead to various damages in fault-crossing tunnels, such as shear damage to the lining, diagonal cracks, axial and transverse damage, and inward deformation[3,4].

Shen et al. [5] demonstrated that flexible joint systems can contain structural damage to specific areas without widespread effects through shaking table tests. Yan et al. [6] improved structural flexibility by incorporating steel-reinforced rubber joints as seismic devices in tunnels, which absorb energy and deformation from earthquakes, thereby enhancing the seismic performance of the structure. Yan et al. [7] studied the damage to tunnels crossing normal faults under the influence of fault misalignment and earthquakes, finding that flexible joints can increase the deformability of tunnel structures, decrease internal forces, and improve seismic performance. AN et al. [8] showed that seismic joints can largely prevent tunnel collapses and highlighted the significance of

W. Nie et al. (eds.), *Proceedings of the 2024 6th International Conference on Hydraulic, Civil and Construction Engineering (HCCE 2024)*, Atlantis Highlights in Engineering 37,
https://doi.org/10.2991/978-94-6463-726-7_75

enhancing the crack resistance and toughness of tunnel lining concrete to reduce the impact of faults.

2 Calculation Model and Loading Method

2.1 Project Overview

This paper relies on the Tajikistan China-Tajikistan Highway Phase II project, tunnel clear width 9.5m, clear height 6.9m, total length 3388m, tunnel site area geomorphology is a high mountainous terrain, the cave body across the ridge, the overall topography of the central high, the two ends of the low, the greatest depth of the tunnel is about 880m. tectonic development of the region of the rock body is broken, the rock layer distribution is uneven, the tunnel geology and tectonics is complex, belongs to the control of the key tunnel project. Fault fracture zone is mainly in the area of V-class surrounding rock, the surrounding rock strength is low, under the action of seismic load tunnel through this area is more likely to suffer greater damage, so this paper focuses on the study of the tunnel through the fault fracture zone.

2.2 Model Scope and Size Case

To examine the seismic dynamic response, a simulation model was constructed. With a depth of around 80 meters, the tunnel is classified as deeply buried. To reduce the calculation's boundary effects, the model's dimensions were expanded laterally by three times the tunnel's diameter (D) on both sides and vertically by D above and below. Measuring 300 meters in length, 120 meters in width, and 120 meters in height, the model incorporates a fault with a 75° dip angle and a 30-meter-wide fault zone. The tunnel has a maximum excavation radius of 5.90 meters, an initial support thickness of 0.25 meters, and a secondary lining thickness of 0.55 meters. The calculation model is depicted in Figure 1.

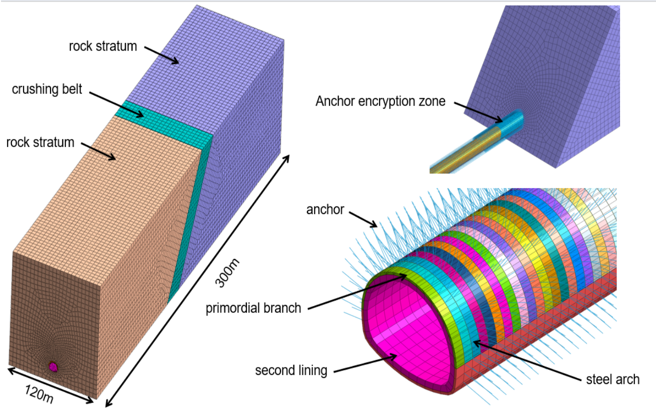

Fig. 1. Model schematic diagram

2.3 Base Material Parameters and Grid Size and Boundary Conditions

Surrounding rock, initial support, secondary lining and fault fracture zone are simulated by solid cells, and the initial support is C25 early-strength concrete, and the secondary lining is C50 concrete. The material parameters of the model are shown in Table 1.

Table 1. Various material parameters of the model

Unit Entity	Density/ $kg{\cdot}m^{-3}$	Modulus of elasticity/GPa	Poisson's ratio	Cohesion /MPa	Angle of internal friction/°
Ordinary perimeter rock	2100	2.50	0.35	0.23	28
Fault fracture zone	1800	0.12	0.40	0.11	21
Grouting layer	2300	8.0	0.25	0.70	37
Initial support	2200	23.0	0.20	-	-
Secondary lining	2500	35.5	0.20	-	-
Steel frame	7850	206	0.25	-	-
Anchor	7850	206	0.25	-	-

2.4 Selection of Seismic Waves and Arrangement of Measurement Points

Given the geological profile of the tunnel, we selected the characteristic EI-Centro seismic waves for dynamic response analysis. T The EI-Centro earthquake had a magnitude of 7.1 and used acceleration data in the vertical upward direction, which was baseline calibrated prior to use of the data. We focused on the first 20 seconds of the seismic waveform, which are representative, and used this segment as input, with the acceleration time history displayed in Figure 2a. To assess the tunnel structure's acceleration and stress responses, a total of 29 monitoring sections were set up along the tunnel's length, covering the entire longitudinal extent. Within each section, eight key monitoring points were identified: the crown, both springing points on the left and right, both waists on the left and right, both bases on the left and right, and the intrados, as shown in Figure 2b.

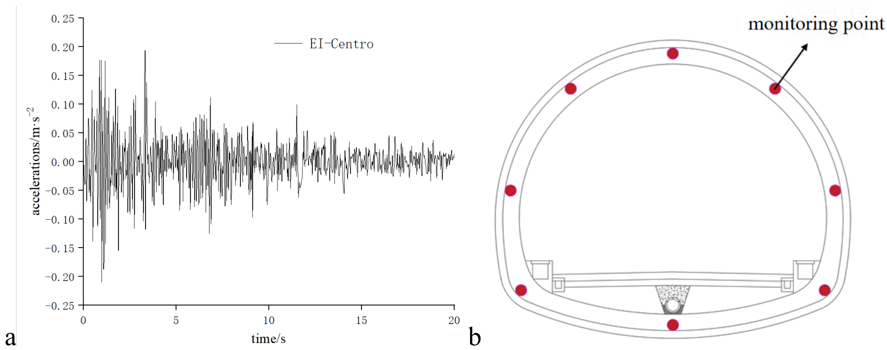

Fig. 2. Seismic wave time profile (a) and site layout (b)

3 Numerical Simulation Analysis

3.1 Acceleration Response Analysis

In seismic assessments, acceleration is crucial for evaluating tunnel structure dynamics. Figure 3a demonstrates that the seismic-induced acceleration of the tunnel lining escalates notably at the fault fragmentation zone, peaking precisely at the fault line. Figure 3b reveals that the vertical acceleration of the tunnel lining within the fault zone experiences an abrupt shift, with the maximum intensity occurring at the fault's core, registering 4.99 m/s². Symmetrical vertical acceleration patterns are evident in the left and right sectors of the tunnel lining's circular cross-section under seismic influence. The augmentation of the tunnel lining's acceleration response is predominantly focused along the tunnel's longitudinal axis, particularly between 120 to 180 meters, where the structure is at higher risk of seismic-induced damage. Enhanced seismic mitigation strategies are recommended for this critical segment.

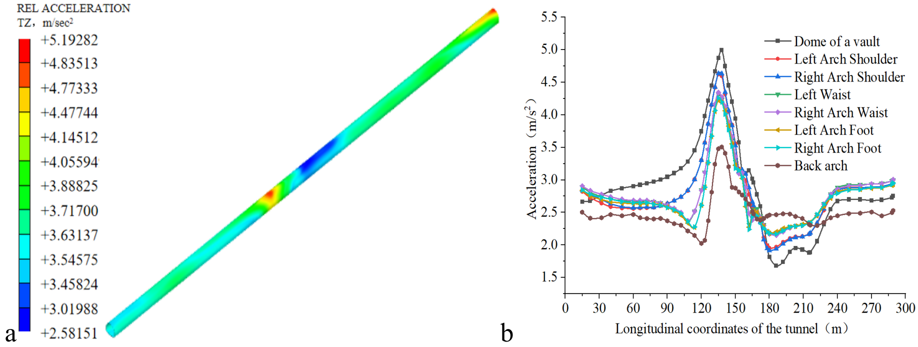

Fig. 3. Acceleration response cloud map (a) and Peak acceleration variation graph (b)

3.2 Stress Response Analysis

A pronounced stress concentration phenomenon is evident in the tunnel lining at the fault fracture zone, where the tunnel lining's maximum and minimum principal stresses (in absolute terms) peak at 5.88MPa and 25.56MPa, respectively. The interval of stress concentration aligns with the intervals of sharp displacement and acceleration changes, mainly between 120 to 180 meters along the tunnel's length. As shown in Figure 4a, the arch waist section has the most significant stress concentration, with the maximum principal stress peaking at 5.88MPa. Figure 4b shows that the arch foot section has the most notable minimum principal stress concentration, which is 13.61 times more concentrated than in the non-fault zone's arch foot, with a maximum value of 25.56MPa in the footing area.

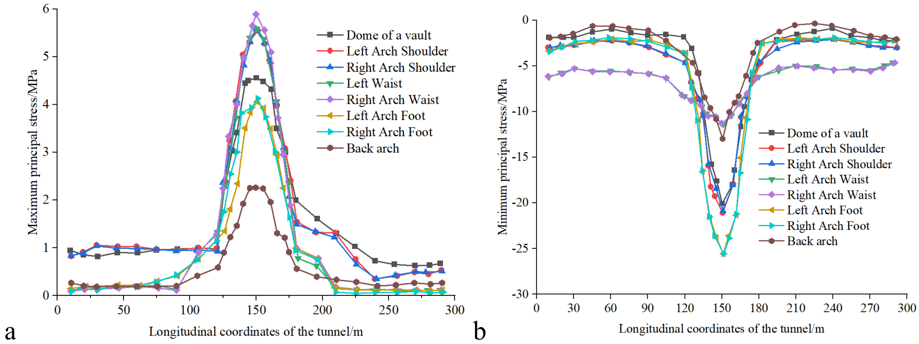

Fig. 4. Maximum principal stress(a) and Minimum principal stress(b)

Comprehensive tunnel lining acceleration and stress along the tunnel axial changes in the situation, should be fault fracture zone and the left and right sides of the range of 30m (about 3 times the diameter of the tunnel) for the seismic protection of the tunnel structure, in this area is easy to lead to the tunnel lining of the disaster phenomenon, seismic protection of the tunnel structure should be used in this range of seismic protection of the corresponding anti-seismic measures.

4 Performance Study of Vibration Damping Measures

The seismic dynamic response is sudden within the fault fracture zone and its primary affected area due to the diminished strength of the surrounding rock and decreased constraints within the fracture zone. This results in heightened seismic loads on the tunnel structure, leading to a "magnification" of structural displacement, maximum shear stress, and maximum principal stress at the fault interfaces. Numerical simulations indicate that anti-seismic measures should be established within a 30-meter perimeter around the fault zone. The proposed deployment strategy includes a sequential setup of "perimeter rock - grouting layer - primary lining - seismic layer - second lining - densely packed anchor rods and steel arch frames."

In a tunnel or underground structure, structural elements such as the surrounding rock, the grouting layer, the primary lining, the damping layer, the secondary lining, the encrypted arrangement of anchors and the encrypted steel arch together form a complex damping system. Grouting layer: a reinforcement layer formed by injecting slurry into the surrounding rock. It can improve the integrity of the surrounding rock, increase the bearing capacity and deformation resistance of the surrounding rock, thus reducing the impact of seismic waves on the tunnel. Seismic damping layer: A rubber layer with low modulus of elasticity is used to increase the flexibility of the structure and reduce the impact of seismic waves on the subsequent structure (secondary lining), thus reducing the dynamic response of the structure. Encrypted arrangement of anchors: can improve the bearing capacity and deformation resistance of the surrounding rock, reducing the displacement and damage caused by the earthquake. Encrypted steel arch: can improve the overall stability and seismic capacity of the support structure. These structures work together to reduce the impact of earthquakes on the tunnel structure by absorbing, dissipating and redistributing the seismic energy to realize the effect of earthquake mitigation.

4.1 Acceleration Response Analysis

Analyzing Figure 5, we find that a tunnel lining equipped with seismic mitigation exhibits comparable behavior to a standard tunnel lining, albeit with a markedly lower degree of change. The maximum vertical acceleration for the tunnel's arch section is noted to be 4.47 m/s², while for the elevated section of the tunnel lining, it is 2.86 m/s². The decrease in peak acceleration for the arch section is 10.51%, and for the elevated section, it is 22.02%. Such reductions are due to the grouting layer's enhancement of the rock conditions surrounding the tunnel's fracture zone, which in turn lessens the seismic-induced displacement there; concurrently, the damping layer's function is to absorb seismic energy, consequently lowering the tunnel's seismic acceleration at the fracture zone.

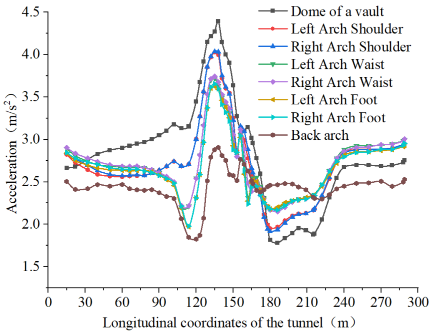

Fig. 5. Acceleration after applying shock absorption measures

4.2 Stress Response Analysis

From Fig. 6, it can be seen that the degree of sudden change in the maximum principal stress of the tunnel lining with anti-seismic measures is smaller than the degree of sudden change in the stress of the conventional tunnel lining. The reason is that under seismic loading, when the tunnel structure in the fault zone undergoes relative displacement and misalignment, it absorbs more energy due to the presence of grouting layer and damping layer. The maximum principal stress peak value of the arch waist part of the tunnel lining is 5.09MPa, and the reduction rate of the arch waist part is 15.52%; the minimum principal stress peak value of the arch foot part of the tunnel lining is 19.56MPa, and the reduction rate is 30.67%. It shows that the maximum principal stress and minimum principal stress response of the tunnel structure at the fault can be greatly reduced by installing anti-seismic measures at the location of the fault fragmentation zone and within the influence range.

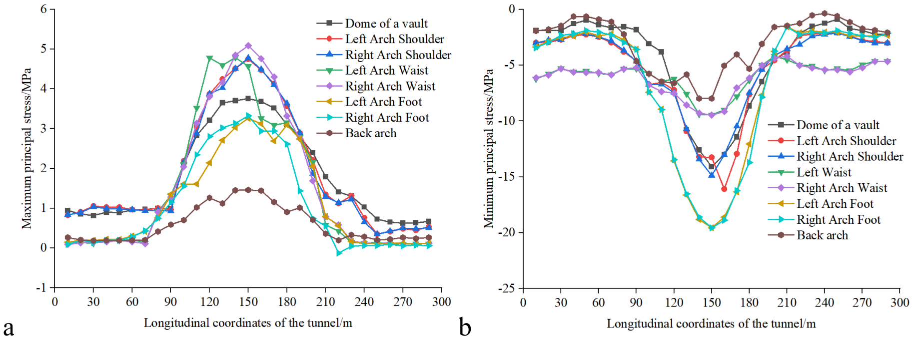

Fig. 6. Maximum principal stress(a) and Minimum principal stress(b)

Although the use of damping measures reduces the acceleration, maximum principal stresses and minimum principal stresses (in absolute terms) in the portion of the tunnel that crosses the fragmentation zone, it increases the stress response in the portion of the tunnel outside the damping structure because the presence of the damping layer may change the force transfer path, causing the portion of the structure farther away from the damping layer to carry more forces. Due to the difference in stiffness between the damping layer and the surrounding rock, the damping layer may transfer some of the seismic forces to other parts of the structure. The damping layer may affect the interaction between the surrounding rock and the lining. In the vicinity of the damping layer, the lining may be subjected to less pressure from the surrounding rock due to the flexibility of the damping layer, which reduces the stresses on the lining. However, outside of the damping layer, the lining may be subjected to more pressure from the surrounding rock, resulting in an increased stress response.

5 Conclusion

With the Sino-Tajikistan Highway Tunnel as the project context and its crossing of a fault fracture zone in mind, this study utilizes numerical simulation to analyze the dynamic response of the tunnel when subjected to earthquakes. The main conclusions drawn are:

1. Under seismic loading, the acceleration and stress response of the tunnel lining at the fault fault zone increases significantly, the stress concentration phenomenon is obvious, and the maximum principal stress and minimum principal stress peak in the fault zone, making the tunnel structure more vulnerable to damage. Acceleration, maximum principal stress and minimum principal stress increase by more than 60% on average in the fault zone area (compared with the non-fault affected area).

2. Through numerical simulation analysis, the damage of tunnel lining in the fault zone is serious, and the fault zone and 30 meters on each side of the fault zone are taken as the key seismic protection area, and the seismic mitigation measures of “peripheral rock - grouting layer - primary lining - damping layer - secondary lining + encrypted arrangement of anchor rods and steel arches” are proposed. Provide a vibration

damping measure for tunnels traversing fractured zones. The peak acceleration, maximum principal stress and minimum principal stress were effectively reduced by 10% after the increase of seismic mitigation measures.

Acknowledgment

Shanxi Provincial Innovation Capability Support Program Project (2020TD-005); 2023 CRBC Science and Technology Research Projects (2023-zlkj-03)

References

1. Sharma, S., & Judd, W. R. (1991). Underground opening damage from earthquakes. *Engineering geology*, *30*(3-4), 263-276. Underground opening damage from earthquakes - ScienceDirect. https://www.sciencedirect.com/science/article/abs/pii/001379529190063Q
2. Asakura, T. (1997, May). Mountain tunnels performance in the 1995 Hyogoken-Nanbu earthquake. In *The 2nd international symposium on recent advances in exploration geophysics (RAEG 1997)* (pp. cp-422). https://www.earthdoc. org/content/papers/10.3997/2352-8265.20140014
3. Kawakami, H. (1984). Evaluation of deformation of tunnel structure due to Izu-Oshima-Kinkai earthquake of 1978. *Earthquake engineering & structural dynamics*, *12*(3), 369-383. https://onlinelibrary.wiley.com/doi/abs/10.1002/eqe.4290120306
4. Geng, P., He, Y., He, C., Quan, Q., & Yan Q. (2014). Research on reasonable aseismic fortified length for tunnel through fault fracture zone. *Chinese Journal of Rock Mechanics and Engineering, 33 (02): 358-365. DOI:10.13722/j.cnki.jrme.2014.02.015.*
5. Shen, Y. S., Wang, Z. Z., Yu, J., Zhang, X., & Gao, B. (2020). Shaking table test on flexible joints of mountain tunnels passing through normal fault. *Tunnelling and Underground Space Technology*, *98*, 103299. https://doi.org/10.1016/j.tust.2020.103299
6. Yan, G., Shen, Y., Gao, B., Zheng, Q., Fan, K., & Huang, H. (2020). Damage evolution of tunnel lining with steel reinforced rubber joints under normal faulting: An experimental and numerical investigation. *Tunnelling and Underground Space Technology*, *97*, 103223. https: //doi. org/10.1016/j.tust.2019.103223
7. An, S., Tao, L. J., Han, X. C., & Zhang, Y. (2021). Application of two-level design method on subway tunnel crossing active fault: a case study on Urumqi subway tunnel intersected by reverse fault dislocation. *Bulletin of Engineering Geology and the Environment*, *80*, 3871-3884. https://doi.org/10.1007/s10064-021-02164-y
8. Zhang, X., Shen, Y. S., Zhou, P. F., & Qiu, J. T. (2023). Partitions of seismic affected zone and characteristics of segmental lining based on energy principle. *Journal of Central South University*, *30*(1), 227-242. https://doi.org/10.1007/s11771-022-5008-7